Optical Frequency Comb Generation and Further Advances From the Photonics Community in Serbia and Western Balkans

Marko M. Krstić [ORCID], Jasna V. Crnjanski [ORCID], and Dejan M. Gvozdić [ORCID]

Abstract—The article presents a short statistical overview of photonics research in the Western Balkans, with more spotlight aimed at the field of optical frequency combs with focus on the overview of the research conducted at the University of Belgrade-School of Electrical Engineering. We give a review of proposed schemes for single and dual optical frequency combs generation, based on optimized gain-switching and electro-optic modulator operation and expand our previous results with analytical approximations for comb lines intensities for the gain-switched laser.

Index Terms—Gain switching, microwave photonics, optical frequency comb, optical signal processing, semiconductor lasers.

I. INTRODUCTION

IN THE domain of modern optics, the development of optical frequency combs (OFCs) has sparked a revolution that transcends traditional boundaries in various scientific and technological domains. The concept of a frequency comb, originating from the field of metrology, i.e., timekeeping experiments [1], has blossomed into a versatile tool with a multitude of applications ranging from fundamental physics to various fields of engineering. The foundation of OFCs can be attributed to the groundbreaking work of Nobel laureate John L. Hall and Theodor W. Hänsch in the early 2000s [2]. Their pioneering research on laser stabilization techniques led to the revelation that a continuous spectrum of equidistant frequency lines could be generated using a mode-locked laser, laying the groundwork for optical frequency combs and opening up a new realm of possibilities in terms of their utilization.

Over the years, in step with constant search for novel applications, the development of OFCs has also progressed along the trajectory of exploration of novel comb generation methods. These methods, including technique of gain-switching [3], use of electro-optic/absorption modulators and micro-resonators [4], [5], and quantum cascade lasers [6], expanded the range of achievable spectral coverage, repetition rates, and comb lines spacing [7]. This diversification of comb sources propelled the development of frequency combs in previously uncharted regions of the electromagnetic spectrum, revolutionizing fields of possible applications, giving rise to OFCs involvement in attosecond physics [8], astrophysics, e.g., for calibration of astronomical spectrographs [9], precise distance measurements [10], but to most extent in spectroscopy [11], where OFCs can serve for direct excitation or interrogation of a sample, and optical telecommunications [12], where they can provide massive parallelizations in wavelength-division multiplexed (WDM) systems, thus meeting the need for constant data rate increase.

In this article we present a short overview on the optical frequency comb research in Western Balkans (Section II), with a focus on the research conducted at the authors' affiliated institution, University of Belgrade-School of Electrical Engineering in Serbia (Section III), dealing with methods of generation and optimization of GHz teeth separation optical frequency combs (Section III-B and III-C) and dual frequency combs (Section III-D), both based on the technique of gain switching. Finally, in the Section IV we give conclusions of the article.

II. OPTICAL FREQUENCY COMB RESEARCH IN WESTERN BALKANS

The Western Balkans (WB) is a designation commonly used for a region which includes Albania, Bosnia and Herzegovina, Croatia, North Macedonia, Montenegro and Serbia. With the exception of Albania, all the countries of the Western Balkans were formerly part of the Socialist Federal Republic of Yugoslavia (SFRY), which dissolved in 1991. Although in this definition Slovenia does not belong to the Western Balkan region, as also formerly part of SFRY, we adopt a wider definition of the WB region, including Slovenia, as depicted in the Fig. 1.

In Fig. 2 we show an overview of number of published research articles [Fig. 2(a)] in journals indexed in Web of Science, and number of their citations [Fig. 2(b)], by country, limited to the research area of optics. Data for Albania and Montenegro are excluded from the figures, due to negligible number of articles/citations. Fig. 2 show that photonics research in the WB region exhibits closely stationary production of research articles in the past 10 years, while the number of citations is in the average decrease from 2016. In the case of Serbia, the share of published articles in the research area of optics in all published articles is between 1–2% in the past 5 years.

The largest and most comprehensive photonics conference in the region is the International School and Conference on
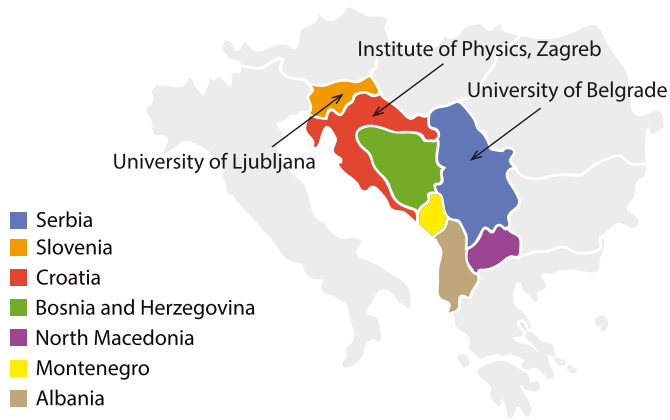
Fig. 1. Western Balkans region comprising Croatia, Bosnia and Herzegovina, Serbia, Montenegro, North Macedonia, Albania, expanded with Slovenia. Map denotes three institutions with ongoing research on optical frequency combs.
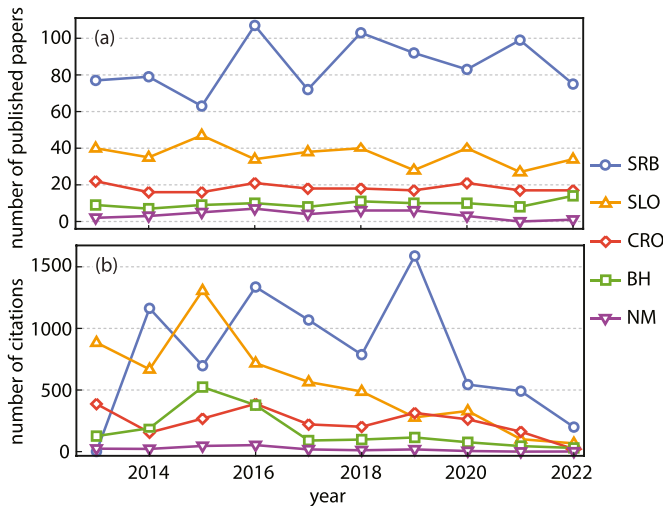

Fig. 2. Number of published articles (a) and citations (b) from 2013 to 2022, for Serbia (SRB), Slovenia (SLO), Croatia (CRO), Bosnia and Herzegovina (BH) and North Macedonia (NM). Statistics include articles published in journals indexed in Web of Science for research area of optics.

Photonics - PHOTONICA [13], held as a biennial event hosted in Belgrade, Serbia since 2007. It is organized by Institute of Physics, Institute of Nuclear Sciences Vinča, Serbian Academy of Sciences and Arts, and Optical Society of Serbia, all with residences in Belgrade, Serbia. The conference covers various subfields of photonics distributed through several sessions: quantum optics and ultra-cold systems, nonlinear optics, optical materials, biophotonics, photonics devices and components, optical communications, laser spectroscopy and metrology, ultrafast optical phenomena, laser-material interaction, optical metamaterials and plasmonics, and from recently machine learning in photonics. The region also organizes and hosts several other conferences which include sessions dedicated to photonics, with most notable being Telecommunications Forum - TELFOR, held yearly in Belgrade with 31 years of tradition, and ETRAN, held yearly since 1955, with venues transferring between the former Yugoslav republics.

The region comprises over 30 universities and significant number of scientific institutes, with photonics research being notably present at Universities of Belgrade, Ljubljana, and Zagreb, Institutes of Physics in Belgrade and Zagreb, Institute Jožef Stefan in Ljubljana, Institute of Nuclear Sciences Vinča in Belgrade, and Institute of Chemistry, Technology and Metallurgy in Belgrade. The research on optical frequency comb in Western Balkans is recognized at three institutions denoted in the Fig. 1, Institute of Physics in Zagreb, Croatia, University of Ljubljana-Faculty of Electrical Engineering, Slovenia, and authors' affiliation institution, University of Belgrade-School of Electrical Engineering, Serbia. The OFCs research at the premises of Institute of Physics, Zagreb is oriented toward atomic and molecular physics, dealing with use of optical frequency combs for atom cooling [14], [15], [16] and inducing radiation pressure force on atoms [17], [18]. The research can be reflected by "Frequency comb cooling of atoms" (CoolComb) project [19], which aims to create the tools that will allow the extension of laser cooling to more diverse species of atoms and molecules, focusing on rubidium (Rb) atoms and two Rb isotopes. On the other hand, the research on OFCs related to University of Ljubljana revolves around techniques of OFC stabilization for further use in the fields of both spectroscopy and optical communications. In particular, the research deals with optical self-injection of single-section semiconductor lasers with quantum dash active region, providing the intermode beat frequency linewidth improvement from 67 kHz to below 900 Hz, indicating the improved optical frequency comb stability [20], [21]. Finally, the OFCs research related to the authors' affiliation institution is discussed in more detail in the following section.

III. OPTICAL FREQUENCY COMB RESEARCH IN SERBIA

The research conducted at the University of Belgrade-School of Electrical Engineering targets optical frequency combs for applications in both optical communications, i.e., combs comprising teeth separation in order of GHz [22], [23], and spectroscopy, requiring order of MHz teeth separation, or dual combs with heterodyne frequencies in the order of kHz [24]. In both cases the research aims to simplify the comb generation scheme exploiting the semiconductor laser gain switching technique with a goal of producing high bandwidth combs with better line flatness. The state-of-the-art approaches for OFC generation include active or passive mode-locked lasers, offering repetition rates from sub-GHz to even THz and bandwidths up to 10 nm, exploiting nonlinear processes in waveguides and microresonators, i.e., Kerr combs, which offer similar repetition rates but bandwidths up to hundreds of nm, and combs residing on the cascade of the laser and electro-optic modulators, offering up to tens of GHz repetition rates and bandwidths up to 200 nm [5]. On the other hand, simple architectures such as gain-switched optical comb sources, although providing lower performance with respect to previously stated techniques, are gaining importance especially for RF photonics applications such as millimeter wave generation, because of their simple and cost-efficient architecture, precisely controlled channel spacing, high level of correlation between the comb lines and low phase noise upon injection

locking with a low linewidth laser. However, the number of comb lines generated directly from a gain-switched laser is limited by the laser's optical bandwidth and the frequency of the drive signal. Typically six comb lines within 3 dB flatness can be obtained when generating an OFC with teeth spacing in order of 10 GHz [25]. Further expansion is usually performed by means of single or multiple external modulators. However, to increase the number of comb lines it is usually necessary to either increase the RF power of the signal driving the modulator and/or use a cascade of modulators, e.g., 38 comb lines with 25 GHz separation by applying 20 V peak-to-peak RF signal to a cascade of one intensity modulator and two phase modulators [26]. Our approach tends to simplify the scheme to a gain-switched laser and one intensity modulator with optimized performance biased with only 1.5 V peak-to-peak RF signal to yield an OFC with 12 comb lines with 9.5 GHz separation [22]. Further simplifications include applying specific optimization techniques to maximize the number of comb lines generated directly from the gain-switched laser where we obtain 7 comb lines with 5 GHz separation [23]. The similar technique has been very recently applied to a scheme with external modulators cascade to obtain 15 lines with 10 GHz spacing [27].

Our second field of interest are dual frequency combs (DFC), which have been verified as a versatile tool for a wide range of applications, especially in the domain of spectroscopy. The state-of-the-art approaches for the DFC generation provide significant capabilities, i.e., combs bandwidths in the order of tens or hundreds of THz, but usually rely on the techniques which are power consuming and in some cases not suitable for photonics integration. These approaches include femtosecond erbium-doped fiber lasers [28], mode-locked erbium fiber ring lasers [29], dissipative Kerr solitons in optical microresonators [30], parametric processes in nonlinear crystals [31], or architectures involving one or several electro-optic modulators [32]. Simpler schemes relying on the mutually injection locked gain-switched lasers have been recently proposed to yield DFCs with bandwidths in order of 100 GHz [33], [34]. Our investigation focuses on the further simplification of the DFC generation scheme based on one laser diode, by designing the adequate temporal form of the driving current pulse for the laser diode large signal modulation [24]. The used temporal forms of the bias current comprise of a train of strong pulses arising from the base current that is above the laser threshold, meaning that the laser is not switched off at any time instance, as opposed to the conventional gain switching techniques. This approach ensures that the photon density and the corresponding phase are unrelated to the spontaneous emission. As a result, this approach not only simplifies the system and enhances power effciency by reducing the number of active components, but also promotes mutual coherence among comb lines, while offering bandwidths in the order of 100 GHz.

A. Model

The gain-switched laser is theoretically modeled as the multiple quantum well distributed feedback (DFB) laser. This modeling considers the laser's dynamics and encompasses the rate equation system, which takes into account carrier transport and parasitic effects [22], thus providing more realistic small and large signal modulation response of the laser. Moreover, this model provides more realistic phase distortions of the emitted light, which we prove to be crucial for the shaping of the comb lines [22]. The model describes the dynamics of the carrier density in the barrier (continuum) states (n_{b}), carrier density in the bound states of the well region (n_{w}), photon density (S) and the optical phase (ϕ):

$$\frac{\mathrm{d}n_{\mathrm{b}}}{\mathrm{d}t} = \frac{\eta_{\mathrm{inj}}I}{qV_{\mathrm{tot}}} - \frac{n_{\mathrm{b}}}{\tau_{\mathrm{b}}} - \frac{n_{\mathrm{b}}}{\tau_{\mathrm{bw}}} + \frac{n_{\mathrm{w}}V_{\mathrm{w}}}{\tau_{\mathrm{wb}}V_{\mathrm{tot}}}. \tag{1}$$

$$\frac{\mathrm{d}n_{\mathrm{w}}}{\mathrm{d}t} = \frac{n_{\mathrm{b}}V_{\mathrm{tot}}}{\tau_{\mathrm{bw}}V_{\mathrm{w}}} - \frac{n_{\mathrm{w}}}{\tau_{\mathrm{w}}} - \frac{n_{\mathrm{w}}}{\tau_{\mathrm{wb}}} - \frac{v_{\mathrm{g}}\Omega(n_{\mathrm{w}}-n_0)S}{1+\varepsilon S}. \tag{2}$$

$$\frac{\mathrm{d}S}{\mathrm{d}t} = \frac{\Gamma v_{\mathrm{g}}\Omega(n_{\mathrm{w}}-n_0)S}{1+\varepsilon S} - \frac{S}{\tau_{\mathrm{p}}} + \Gamma\frac{R_{\mathrm{sp}}}{V_{\mathrm{tot}}}. \tag{3}$$

$$\frac{\mathrm{d}\phi}{\mathrm{d}t} = \frac{1}{2}\alpha\left(\frac{\Gamma v_{\mathrm{g}}\Omega(n_{\mathrm{w}}-n_0)}{1+\varepsilon S} - \frac{1}{\tau_{\mathrm{p}}}\right). \tag{4}$$

Parameters from the equations above are fitted to correspond to the dynamics of the available commercial, high-speed DFB laser (Gooch & Housego AA0701 series InGaAsP/InP multi-quantum well distributed feedback laser diode) with high modulation bandwidth [22]. The output slowly varying envelope of the gain-switched laser electrical field E_{gs} of the resulting output field is expressed as:

$$E_{\mathrm{gs}}(t) = \sqrt{S(t)}e^{-i\phi(t)}. \tag{5}$$

Our research revolves around two schemes of comb generation: by means of a single gain-switched laser, with optimization of the modulating current waveform aiming for increase in the bandwidth and flatness of the resulting comb, and by cascading the gain-switched laser with dual-drive Mach-Zender modulator (DD-MZM), with optimization of the modulator operation. In the analysis of the latter, we use the standard transfer function of the DD-MZM [22] which gives the slowly varying envelope of the output electrical field after the DD-MZM stage as:

$$E_{\mathrm{out}}(t) = (1/2)E_{\mathrm{gs}}(t)\left[e^{i\varphi_1(t)} + e^{i\varphi_2(t)}\right]. \tag{6}$$

Here, $\varphi_1(t)$ and $\varphi_2(t)$ stand for induced phases in the modulator arms with respect to applied arm voltages v_1 and v_2, i.e., $\varphi_1(t) = (\pi/V_\pi)v_1(t)$, and $\varphi_2(t) = (\pi/V_\pi)v_2(t)$, where V_π denotes the switching bias voltage of the DD-MZM. Substituting this into (6) gives:

$$E_{\mathrm{out}}(t) = E_{\mathrm{gs}}(t)\cos\left[\frac{\pi}{2V_\pi}(v_1-v_2)\right]e^{i\frac{\pi}{2V_\pi}(v_1+v_2)}. \tag{7}$$

In our analysis, we apply simple harmonic voltages to DD-MZM arms $v_1(t) = V_{\mathrm{DC}} + V_{\mathrm{RF}}\cos(2\pi f_{\mathrm{MZM}}t)$ where V_{DC} and V_{RF} define the quiescent point and modulation depth, respectively, while f_{MZM} denotes the frequency at which MZM is modulated. Furthermore, we assume push-pull configuration, so that $v_2(t) = -v_1(t)$. Substituting this into the (7) shows that this leads to the pure intensity modulation, i.e., the original phase of

E_{gs} stays preserved and (7) can be written as:

$$E_{\mathrm{out}}(t) = E_{\mathrm{gs}}(t) \cos\left[\eta + \xi \cos(2\pi f_{\mathrm{MZM}}t)\right], \qquad (8)$$

with $\eta = \pi V_{\mathrm{DC}}/V_\pi$ and $\xi = \pi V_{\mathrm{RF}}/V_\pi$. By decomposing the cosine of the sum of two angles in the (8) and expanding in series of Bessel functions [35], the last equation can be rewritten as:

$$
\begin{aligned}
E_{\mathrm{out}}(t) = E_{\mathrm{gs}}(t) \\
\times \Bigg\{ & \left[\cos(\eta)\left(J_0(\xi) + 2\sum_{k=1}^{\infty}(-1)^k J_{2k}(\xi)\cos(2k2\pi f_{\mathrm{MZM}}t)\right)\right] \\
& - \left[\sin(\eta)\left(-2\sum_{k=1}^{\infty}(-1)^k J_{2k-1}(\xi)\cos((2k-1)2\pi f_{\mathrm{MZM}}t)\right)\right]\Bigg\},
\end{aligned}
$$
$$(9)$$

where J_k denotes Bessel function of the first kind. The equation shows that the electrical field obtained by the gain switching E_{gs} is further intensity modulated with harmonics which are weighted with Bessel functions. Moreover, it can be noted that even harmonics are weighted by even order Bessel functions, while odd harmonics are weighted by odd order Bessel functions. By setting the quiescent point, i.e., factor η, even or odd harmonics could be suppressed, provided that $\cos(\eta) = 0$ or $\sin(\eta) = 0$. The final optical phase of the resulting electrical field E_{out} corresponds to the original optical phase of the gain switched laser field E_{gs}, which can be obtained from the rate equation (4). The output frequency comb is obtained as the Fourier transform of the slowly varying electrical field envelope $E_{\mathrm{gs}}(t)$ or $E_{\mathrm{out}}(t)$, depending on the applied scheme. Harmonics of such defined comb are obtained relative to the fundamental frequency of the laser diode.

B. GHz Teeth OFCs: Cascade of Gain-Switched Laser and Dual-Drive MZM

In the gain switching stage, the laser is driven by the sinusoidal electrical current in the form:

$$I(t) = c_0 + \sum_{h=1}^{N} |c_h| \sin(2\pi h f_{\mathrm{gs}}t + \varphi_h), \qquad (10)$$

where N stands for the number of harmonics constituting the bias current waveform, c_0 stands for the constant bias current, c_h and φ_h for the amplitudes and phases of the harmonics, and f_{gs} for the fundamental frequency of the gain switching. Our theoretical analysis shows that in the case of the gain switching by means of simple harmonic bias current, i.e., $N = 1$, flat-top optical comb can be obtained when the current amplitudes c_0 and c_1 provide that the output optical phase $\phi(t)$ of the gain-switched laser oscillates very close to a simple harmonic function (sine/cosine) with peak-to-peak amplitude close to π. This can be shown by taking the optical phase as $\phi(t) = \phi_0 + \Delta\phi \sin(2\pi f_{\mathrm{gs}}t + \theta)$, with ϕ_0 being a phase offset, $\Delta\phi$ an amplitude of the phase oscillation (with value which should be close to $\pi/2$) and θ the phase of the sine function. Without compromising the generality of the derived conclusions, the phase θ can be taken as arbitrary, so we take $\theta = 0$. The output slowly varying envelope of the electrical field obtained after the

gain switching (5) can be now represented as:

$$E_{\mathrm{gs}}(t) = \sqrt{S(t)}\, e^{-i\phi_0} e^{-i\Delta\phi \sin(2\pi f_{\mathrm{gs}}t)}. \qquad (11)$$

Expanding the amplitude $\sqrt{S(t)}$ in Fourier series and $e^{-i\Delta\phi \sin(2\pi f_{\mathrm{gs}}t)}$ term by means of Jacobi-Anger expansion [35] we get:

$$
\begin{aligned}
E_{\mathrm{gs}}(t) &= \left(\sum_{n=-\infty}^{\infty} a_n e^{i2\pi n f_{\mathrm{gs}}t}\right) e^{-i\phi_0} e^{-i\Delta\phi \sin(2\pi f_{\mathrm{gs}}t)} \\
&= e^{-i\phi_0} \sum_{n=-\infty}^{-\infty} a_n e^{i2\pi n f_{\mathrm{gs}}t} \sum_{m=-\infty}^{-\infty} J_m(-\Delta\phi) e^{i2\pi m f_{\mathrm{gs}}t} \\
&= e^{-i\phi_0} \sum_{n=-\infty}^{-\infty} a_n e^{in\omega_{\mathrm{gs}}t} \sum_{m=-\infty}^{-\infty} J_m(-\Delta\phi) e^{im\omega_{\mathrm{gs}}t},
\end{aligned}
$$
$$(12)$$

where $\omega_{\mathrm{gs}} = 2\pi f_{\mathrm{gs}}$. The form of E_{gs} given by (12) can be further decomposed in a way that coefficients comprised of products between a_n and $J_m(-\Delta\phi)$, standing in front of an appropriate harmonic ($e^{inm\omega_{\mathrm{gs}}t}$ term) can be recognized and grouped. Such decomposition provides analytical formulae for every particular harmonic of E_{gs}, i.e., comb line, with its intensity being defined by squared absolute value of the coefficient related to the particular harmonic. We present E_{gs} harmonic decomposition:

$$
\begin{aligned}
E_{\mathrm{gs}}(t) &= e^{-i\phi_0} \sum_{k=-\infty}^{\infty} L_k e^{ik\omega_{\mathrm{gs}}t} \\
&= e^{-i\phi_0}(L_0 + L_1 e^{i\omega_{\mathrm{gs}}t} + L_{-1} e^{-i\omega_{\mathrm{gs}}t} \\
&\quad + L_2 e^{i2\omega_{\mathrm{gs}}t} + L_{-2} e^{-i2\omega_{\mathrm{gs}}t} \\
&\quad + L_3 e^{i3\omega_{\mathrm{gs}}t} + L_{-3} e^{-i3\omega_{\mathrm{gs}}t}\cdots).
\end{aligned}
$$
$$(13)$$

in which we address seven comb lines: the central line, corresponding to the fundamental frequency of the laser, with magnitude defined by $|e^{-i\phi_0}L_0|^2$, and three lines on the each spectrum side, with angular frequencies separated from the central line by $\pm\omega_{\mathrm{gs}}$, $\pm2\omega_{\mathrm{gs}}$, and $\pm3\omega_{\mathrm{gs}}$, with magnitudes defined by $|e^{-i\phi_0}L_{\pm1}|^2$, $|e^{-i\phi_0}L_{\pm2}|^2$, and $|e^{-i\phi_0}L_{\pm3}|^2$, respectively. Taking into account that coefficients a_n are obtained from a Fourier series of a real-valued function $\sqrt{S(t)}$, so they follow the symmetry $a_1 = a_{-1}, a_2 = a_{-2}, \ldots$, and applying the relations valid for integer order Bessel functions, $J_m(-\Delta\phi) = (-1)^m J_m(\Delta\phi)$ and $J_{-m}(-\Delta\phi) = (-1)^m J_m(-\Delta\phi)$, we present the analytical expressions for L coefficients, in which we neglect the influence of coefficients a_n with order higher than 3:

$$L_0 = a_0 J_0(\Delta\phi) + 2a_2 J_2(\Delta\phi) + 2a_4 J_4(\Delta\phi), \qquad (14a)$$

$$
\begin{aligned}
L_1 = {} & -a_0 J_1(\Delta\phi) + a_1\left[J_0(\Delta\phi) + J_2(\Delta\phi)\right] \\
& + a_2\left[J_1(\Delta\phi) - J_3(\Delta\phi)\right] + a_3\left[J_2(\Delta\phi) + J_4(\Delta\phi)\right],
\end{aligned}
$$
$$(14b)$$

$$
\begin{aligned}
L_{-1} = {} & a_0 J_1(\Delta\phi) + a_1\left[J_0(\Delta\phi) + J_2(\Delta\phi)\right] \\
& + a_2\left[-J_1(\Delta\phi) + J_3(\Delta\phi)\right] + a_3\left[J_2(\Delta\phi) + J_4(\Delta\phi)\right],
\end{aligned}
$$
$$(14c)$$

$$L_2 = a_0 J_2(\Delta\phi) + a_1 \left[-J_1(\Delta\phi) - J_3(\Delta\phi) \right]$$
$$+ a_2 \left[J_0(\Delta\phi) + J_4(\Delta\phi) \right] + a_3 \left[J_1(\Delta\phi) - J_5(\Delta\phi) \right], \tag{14d}$$

$$L_{-2} = a_0 J_2(\Delta\phi) + a_1 \left[J_1(\Delta\phi) + J_3(\Delta\phi) \right]$$
$$+ a_2 \left[J_0(\Delta\phi) + J_4(\Delta\phi) \right] + a_3 \left[-J_1(\Delta\phi) + J_5(\Delta\phi) \right], \tag{14e}$$

$$L_3 = -a_0 J_3(\Delta\phi) + a_1 \left[J_2(\Delta\phi) + J_4(\Delta\phi) \right]$$
$$+ a_2 \left[-J_1(\Delta\phi) - J_5(\Delta\phi) \right] + a_3 \left[J_0(\Delta\phi) + J_6(\Delta\phi) \right], \tag{14f}$$

$$L_{-3} = a_0 J_3(\Delta\phi) + a_1 \left[J_2(\Delta\phi) + J_4(\Delta\phi) \right]$$
$$+ a_2 \left[J_1(\Delta\phi) + J_5(\Delta\phi) \right] + a_3 \left[J_0(\Delta\phi) + J_6(\Delta\phi) \right] \tag{14g}$$

For simple harmonic gain switching, the coefficient a_0 dominates over higher order coefficients by an order of magnitude. By inspection of the comb line expressions (14), it can be noted that coefficients L_0, L_1, and L_{-1} would exhibit equalized contribution of a_0 for $J_0(\Delta\phi) = J_1(\Delta\phi)$, which holds for $\Delta\phi = \Delta\phi_0 \approx 1.4347$ rad. In this case, Bessel functions of 3rd and higher orders are close to 0 so they can be neglected (expect when multiplied by a_0). In the second order of approximation, all contributions expect the dominant can be neglected, leading to simple expressions for comb lines, predicting the three flat line comb:

$$L_0 = a_0 J_{0/1} + 2a_2 J_2 \approx a_0 J_{0/1}, \tag{15a}$$

$$L_1 = -a_0 J_{0/1} + a_1 \left(J_{0/1} + J_2 \right) + a_2 J_{0/1} + a_3 J_2$$
$$\approx -a_0 J_{0/1}, \tag{15b}$$

$$L_{-1} = a_0 J_{0/1} + a_1 \left(J_{0/1} + J_2 \right) - a_2 J_{0/1} + a_3 J_2$$
$$\approx a_0 J_{0/1}, \tag{15c}$$

$$L_2 = a_0 J_2 - a_1 J_{0/1} + a_2 J_{0/1} + a_3 J_{0/1} \approx a_0 J_2, \tag{15d}$$

$$L_{-2} = a_0 J_2 + a_1 J_{0/1} + a_2 J_{0/1} - a_3 J_{0/1} \approx a_0 J_2, \tag{15e}$$

$$L_3 = -a_0 J_3 + a_1 J_2 - a_2 J_{0/1} + a_3 J_{0/1} \approx -a_0 J_3, \tag{15f}$$

$$L_{-3} = a_0 J_3 + a_1 J_2 + a_2 J_{0/1} + a_3 J_{0/1} \approx a_0 J_3, \tag{15g}$$

where we introduce notation $J_0(\Delta\phi_0) = J_1(\Delta\phi_0) = J_{0/1}$ and $J_2(\Delta\phi_0) = J_2$.

The schematic concept of the gain-switched comb further expansion is given in the Fig. 3. In the gain switching stage we obtain the three flat lines comb, as predicted by the presented analytics, while the task of the modulator is to create spectrum replicas and shift them to higher and lower frequencies with respect to the original spectrum, thus expanding the number of strong lines in the final stage. In the proposed scheme, we bias the DD-MZM with $V_{DC} = V_\pi$ which makes $\sin(\eta) = 0$ in the (9), suppressing the odd MZM harmonics. Furthermore, we set the RF voltage to equate the power of the fundamental MZM harmonic with the first even MZM harmonic (MZM harmonic ± 2), by equating the corresponding Bessel functions $|J_0(\xi)| = |J_2(\xi)|$ which is feasible for $\xi = 0.586\pi$
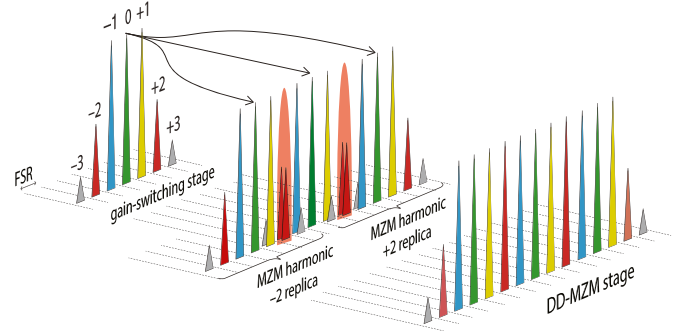

Fig. 3. Schematic concept of the gain switched comb expansion. Three flat lines frequency comb generated after the gain switching stage. The symmetrical distribution of the side-comb lines (lines ± 2) is feasible for simple harmonic optical phase modulation profile. Expansion of the comb after the DD-MZM stage. MZM harmonics ± 2 produce spectrum replicas which contribute to expansion of the final comb to 11 flat lines. The arrowed lines depict the directions of mappings between the original spectrum and its replicas due to MZM expansion. Flatness of the expanded comb crucially depends on the summation of the lines -2 and $+2$ between original spectrum and its replicas. Reprinted with permission from [22] © The Optical Society.

i.e., $V_{RF} = 0.586 V_\pi$, making this scheme power efficient. In this case, higher even MZM harmonics (harmonics ± 4, ± 6,...) are significantly suppressed as the values of the higher Bessel functions ($J_4(\xi)$, $J_6(\xi)$,...) are approximately zero. In order to replicate the laser comb spectrum and to shift it, we modulate the MZM by modulation frequency f_{MZM} which shifts the replicas of the spectrum by $4 f_{gs}$. Since we use the second MZM harmonic, the necessary frequency of the MZM modulation is given by $f_{MZM} = 4 f_{gs}/2 = 2 f_{gs}$. In this way, the spectrum replica originating from the MZM harmonic -2, produces the overlapping of the comb line $+2$ from the spectrum replica, with the comb line -2 from the original spectrum (overlapping of the two red comb lines shown in the Fig. 3). On the other side, the spectrum replica originating from the MZM harmonic $+2$, produces the overlapping of the comb line -2 from the spectrum replica, with the comb line $+2$ from the original spectrum. The final comb consists of $3 \times 3 = 9$ flat lines as the result of direct replicas of the initial spectrum, plus 2 additional lines as the result of the overlapping. In the case in which overlapping produces comb lines with similar power to the initially flat ones, the final comb can be comprised of 11 flat comb lines. Indeed, the analytical expressions for comb lines ± 2 (15d) and (15e), predict the feasibility of such scenario as $J_0(\Delta\phi_0) \approx 2.5 J_2(\Delta\phi_0)$.

It should be noted that $\xi \approx 3.14\pi$ i.e., $V_{RF} \approx 3.14 V_\pi$ could yield $|J_0(\xi)| \approx |J_2(\xi)|| \approx |J_4(\xi)|$ which could add two more replicas originating from the MZM harmonics ± 4. In this case our scheme predicts 19 flat lines, 15 lines corresponding to 5 replicas of the initially 3 flat lines, plus 2 lines resulting from overlapping of the original spectrum with second MZM harmonic, and 2 lines resulting from overlapping of the second and fourth MZM harmonic.

Proposed theory has been experimentally confirmed in cooperation with the Dublin City University, Laboratory for Radio and Optical Communications, Ireland, and presented in [22]. Fig. 4 presents the results of the experiment and shows the output spectrum of the dual stage comb source when both
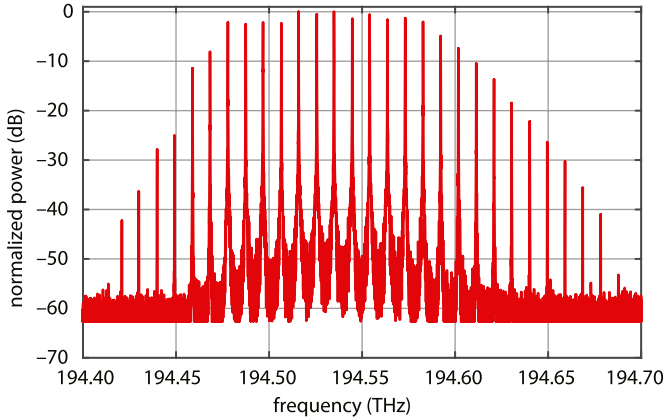
Fig. 4. Two-stage comb source output spectrum with 12 lines in 3 dB flatness and FSR of 9.5 GHz. Reprinted with permission from [22] © The Optical Society.

gain switching laser and DD-MZM are under modulation with $f_{gs} = 9.5$ GHz, while DD-MZM parameters follow the scenario envisioned by the theory ($f_{MZM} = 2f_{gs}$, $V_{DC} = V_\pi$ and $V_{RF} = 0.586V_\pi \approx 1.5$ V). Twelve lines within 3 dB flatness, constituting a total bandwidth of 105 GHz, are obtained with an FSR of 9.5 GHz and a carrier to noise ratio of around 42 dB. It should be noted that the number of comb lines obtained by experiment (12) is increased in comparison with conceptually predicted number (11). The reason for this lies in the nonlinear phase distortion, i.e., deviation from the pure sine form, and corresponding laser spectrum asymmetry, and is explained in more detail in [22].

C. GHz Teeth Separation OFCs: Optimization of the Gain-Switched Laser Bias Current Waveform

In the other approach, developed in the cooperation with Department of Electrical and Photonics Engineering at DTU, Denmark, the potential capability of the laser alone, i.e., without any modulator in the setup, is explored to improve the OFC characteristics in terms of flatness and bandwidth [23]. For that, in order to promote the higher-order harmonics in the gain-switched spectrum, multiple harmonics are considered in $I(t)$, (10), with magnitude of the bias current c_0, the amplitudes c_h, and the phases ϕ_h of the harmonics being subjected to optimization methods using gradient-free algorithms, such as particle swarm optimization (PSO) and differential evolution (DE) algorithms. The target was set to minimize the flatness margin of a defined number of OFC lines.

Fig. 5 [23] shows the optimized OFCs based on the application of DE and PSO algorithms to the laser model (1)–(4). Presented results constitute the best OFCs spectra achieved in terms of combined flatness and the number of lines for the presented DFB laser model, for fundamental modulation frequency $f_{gs} = 5$ GHz. For the case of $I(t)$ composed of three harmonics [$N = 3$ in (10)], a 9-lines OFC (40 GHz span) is achieved with 2.9 dB and 3.3 dB flatness for the DE and PSO algorithms, respectively [Fig. 5(a) and (b)]. With fewer parameters optimization, the DE OFC flatness optimization for the single harmonic laser driving

signal is shown in Fig. 5(c), yielding in 9-lines OFC with 5.7 dB flatness. The PSO case is not presented for $N = 1$ due to similar results as for the DE case. These results confirm the benefits to the OFC flatness of applying harmonic superposition to the laser driving signal when combined with an optimization algorithm.

In the experimental proof-of-concept of the proposed method [23], the single harmonic ($N = 1$) and three harmonics ($N = 3$) cases were considered for the laser driving signal. It should be noted that the used high modulation bandwidth laser (NLK1551SSC) differs from the one stated in the model. The optimization was performed online, directly on the laser under test without any previous or posterior offline processing. The OFC was captured using a high-resolution optical spectrum analyzer and OFC output features were optimized by the means of DE algorithm which controlled signal generators and power supply outputs, constituting the bias current waveform. Fig. 6 shows experimentally obtained spectra, representing averages from 50 measurements in 1 s time interval, for optimization of one harmonic bias current [Fig. 6(a)], three harmonics bias current with features including only current amplitudes [Fig. 6(b)], and three harmonics bias current with full feature set, comprising of current harmonics amplitudes and phases [Fig. 6(c)]. The fundamental modulation frequency f_{gs} in the presented case is 5 GHz, as in the theoretical approach. The obtained results are, respectively, 5-lines OFC with $\sim$7.1 dB flatness, 6-lines OFC with $\sim$3 dB flatness, and 7-lines OFC with $\sim$2 dB flatness. In case of [Fig. 6(c)], taking the set of 9 lines, as in theoretical approach, the obtained flatness is higher than predicted by the model, $\sim$6 dB. Experimental implementation showed that good flatness values can be obtained already after 30 iterations of the applied optimization algorithm, after which the flatness keeps slightly improving towards the end of the optimization (100 iterations in average). This characteristic can be explored for faster optimization, depending on the target OFC.

D. Dual OFCs

The model of the laser correspond to the model given by (1)–(4). The laser diode is driven by electrical current $I(t)$ representing the superposition of two wave-forms with close-valued frequencies:

$$ I(t) = I_b + h(t) \sum_{k=1}^{2} \Delta I \left[\frac{\sin(2\pi N f_k t)}{N \sin(2\pi f_k t)} \right]^p, \quad (16) $$

where I_b stands for the bias current, ΔI for the amplitude of modulation, f_1 and f_2 are two close-valued modulation frequencies ($f_2 = f_1 + \delta f$, $\delta f \ll f_1$), while h denotes the Heaviside step function, i.e., modulation starts after the laser has stabilized its continuous wave output. Finally, parameter N defines the electrical current spectrum bandwidth $B = N f_2$. In our simulations we use odd values of N, since in this case the current wave-form consists of positive current spikes providing better shaped DFCs. In our work we analyze two forms of the electrical current, the one comprising of the sum of two trains of $sinc$ pulses, obtained for $p = 1$, and the second, comprising of the sum of two trains of $sinc^2$ pulses, obtained for $p = 2$. Apart from differences in the shape of the output DFCs in
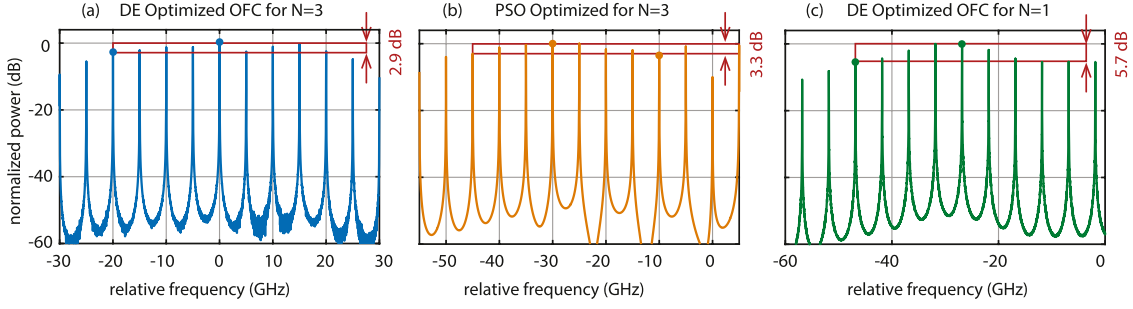
Fig. 5. Optimized GS-laser 9-line OFCs with different flatness obtained for single harmonic laser driving signal ($N = 1$) and multiple harmonics laser driving signal ($N = 3$). Relative frequency is given with respect to the lasing frequency. Reprinted with permission from [23] © The Optical Society.
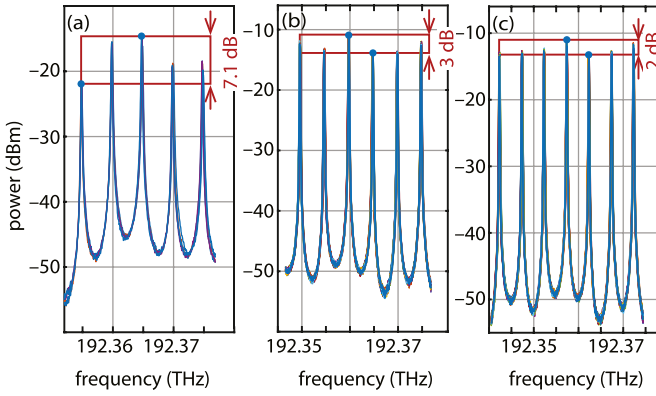

Fig. 6. Experimental OFC optimized (averaged flatness of 50 measured spectra overlapped) using DE algorithms for: (a) one harmonic in the laser driving signal (5 lines in ~7.1 dB), (b) three harmonics in the laser driving signal, with optimization of the amplitudes (6 lines in ~3 dB), and (c) three harmonics in the laser driving signal, with optimization of amplitudes and phase differences (7 lines in ~2 dB). Reprinted with permission from [23] © The Optical Society.

terms of span and flatness, cases $p = 1$ and $p = 2$ also differ in terms of comb teeth separation. In case of $p = 1$, the resulting output DFC consists of series of teeth pairs (t.p.) appearing at $\pm 2n \times (f_1 + f_2)/2$, relative to the central lasing frequency, where n denotes the ordinal of the teeth pair with respect to the central comb line. The heterodyne frequency of the nth teeth pair is equal to $2n \times (f_2 - f_1) = 2n \times \delta f$. In the other case ($p = 2$), t.p. separation and heterodyne frequencies are halved. For that matter, in case $p = 1$ we take $f_1 = 100$ MHz, $\delta f = 0.25$ MHz, while for $p = 2$, we take doubled values, in order to obtain same teeth pairs separation and heterodyne frequencies in both cases.

In both cases we analyze the influence of the applied current bandwidth B, magnitudes of the bias current and modulation amplitude, I_b and ΔI, respectively, and value of the linewidth enhancement factor α on the formation of the DFCs. As one of the figures of merit we take the comb span, which we define as the number of teeth pairs in the defined power margin. Here we exclude the central line, which is highly pronounced in both DFC cases. For the reference power margin we take 20 dB, measured from the teeth pair with highest power. In addition, we discuss the optical power per teeth pair and define the spectrum power efficiency (SE) as the ratio of power distributed into teeth pairs with respect to the total power.
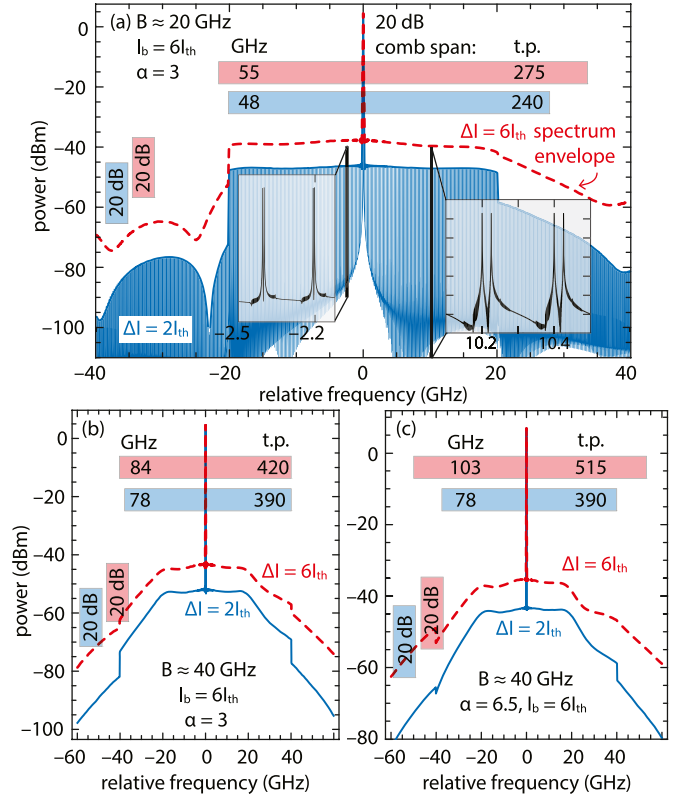

Fig. 7. DFCs for (a) $\alpha = 3$ and (b)–(c) $\alpha = 6.5$ and two amplitudes of modulation, $\Delta I = 2I_{th}$ (solid lines) and $6I_{th}$ (dashed lines), for electrical current bandwidth (a) $B \approx 20$ GHz and (b)–(c) $B \approx 40$ GHz. Shaded rectangles denote dual frequency comb 20 dB span expressed in GHz and as number of teeth pairs (t.p.). Insets in (a) provide more clear visualisation of the comb lines arrangements. Right inset shows zoom of 51st and 52nd teeth pair on the positive spectrum side, with heterodyne frequencies corresponding to 25.5 and 26 MHz, respectively, while left inset shows zoom of 11th and 12th teeth pair on the negative spectrum side, with heterodyne frequencies corresponding to 5.5 and 6 MHz, respectively. Reprinted with permission from [24] © The Optical Society.

We show that in case of $sinc$-shaped pulses ($p = 1$), with $B \approx 20$ GHz, lower α, and for moderate I_b and small modulation amplitude ΔI, smaller output DFCs spans of 40 GHz can be obtained with high level of comb line flatness, in order of 1 dB, with power per pair of 60 nW, as depicted with blue solid line in Fig. 7(a) (span from -20 to 20 GHz) [24]. If
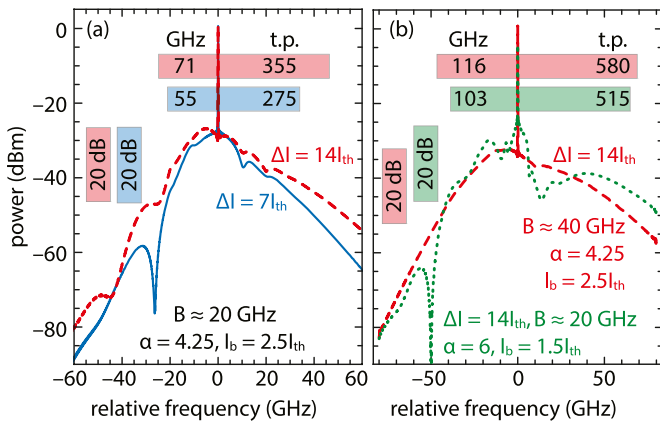
Fig. 8. DFCs envelopes for bias currents $I_b = 1.5I_{th}$, $2.5I_{th}$ and $\Delta I = 7I_{th}$ (solid line) and $14I_{th}$ (dashed and dotted lines). (a) Envelopes for $\alpha = 4.25$ all for $B \approx 20$ GHz. (b) Envelopes for $\alpha = 4.25$, $I_b = 2.5I_{th}$ and $B \approx 40$ GHz (dashed line) and for $\alpha = 6$, $I_b = 1.5I_{th}$, $B \approx 20$ GHz (dotted line), all for $\Delta I = 14I_{th}$. Reprinted with permission from [24] © The Optical Society.

taking 20 dB margin merit (denoted by the shaded rectangle) comb span is somewhat higher, 48 GHz, i.e., 240 teeth pairs. Larger amplitudes of modulation can raise the maximal power per teeth pair for an order of magnitude, as well as the comb span according to 20 dB criterion, however on the expense of somewhat disturbed line flatness in ±20 GHz region (instead of depicting the whole comb, we present the spectrum envelope, denoted in red, dashed line in Fig. 7(a)]. Larger bias current bandwidth lowers the maximal power in teeth pairs [Fig. 7(b)] in comparison with spectra presented in Fig. 7(a), but contributes to larger 20 dB comb span. However, the flatness of the lines is still preserved in the same span, from −20 to 20 GHz. A laser diode with higher α, although comprising pronounced phase noise, can significantly raise the maximal power per t.p. and contribute to higher comb span [e.g., 103 GHz, red dashed line in Fig. 7(c)]. However, in all presented cases, the spectrum efficiency is low, in the order of $SE \approx 1-3\%$.

The current wave-form comprising of $sinc^2$ shaped pulses can significantly raise the SE in comparison to the case of the $sinc$ pulses, on the expense of highly distorted comb flatness, and requires much higher amplitudes of modulation and, taking into account the current limits of the laser, lower bias currents. In Fig. 8 we present comb envelopes for different parameters of modulation and different values of α in case of the $sinc^2$ shaped pulses modulation. For lower values of α, SE is in the range from 15% to 25%, with lower values corresponding to the case of higher bandwidth B. On the other hand, higher values of α in combination with lower I_b and B [green, dotted line in Fig. 8(b)] can increase SE up to 52%, as well as the maximal power per teeth, and consequently the comb span. However, the largest span is obtained in case of higher I_b and B, for lower α, yielding 116 GHz (580 t.p.) with maximal power per pair of 1.3 μW and $SE = 15\%$ [red, dashed line in Fig. 8(b)].

IV. CONCLUSION

The article presents a short statistical overview of the photonics research in the Western Balkan countries, which exhibits a steady-state journal articles production in the last 10 years window. Furthermore, we give a short remarks on the optical frequency comb research in the region, and focus on the research conducted at University of Belgrade-School of Electrical Engineering. In the short review of this work, we present the analytical approximations for comb lines intensities in gain-switched laser and two power efficient techniques for further comb expansion, via tailoring the form of the laser bias current, by means of optimization algorithms, or cascading the dual-drive Mach-Zender modulator with optimized bias. Finally, we present the tailored wave-forms of the laser bias current and show methods for generation of dual combs by means of a single laser diode.

REFERENCES

[1] L. Essen and J. V. L. Parry, "An atomic standard of frequency and time interval: A cæsium resonator," *Nature*, vol. 176, pp. 280–282, 1955.
[2] T. W. Hänsch, "Nobel lecture: Passion for precision," *Rev. Modern Phys.*, vol. 78, pp. 1297–1309, 2006.
[3] K. Y. Lau, "Gain switching of semiconductor injection lasers," *Appl. Phys. Lett.*, vol. 52, pp. 257–259, 1988.
[4] A. L. Gaeta, M. Lipson, and T. J. Kippenberg, "Photonic-chip-based frequency combs," *Nature Photon.*, vol. 13, pp. 158–169, 2019.
[5] L. Chang, S. Liu, and J. E. Bowers, "Integrated optical frequency comb technologies," *Nature Photon.*, vol. 16, pp. 95–108, 2022.
[6] J. Faist et al., "Quantum cascade laser frequency combs," *Nanophotonics*, vol. 5, pp. 272–291, 2016.
[7] T. Fortier and E. Baumann, "20 years of developments in optical frequency comb technology and applications," *Commun. Phys.*, vol. 2, 2019, Art. no. 153.
[8] A. Baltuška et al., "Attosecond control of electronic processes by intense light fields," *Nature*, vol. 421, pp. 611–615, 2003.
[9] T. Wilken et al., "A spectrograph for exoplanet observations calibrated at the centimetre-per-second level," *Nature*, vol. 485, pp. 611–614, 2012.
[10] I. Coddington, W. C. Swann, L. Nenadović, and N. R. Newbury, "Rapid and precise absolute distance measurements at long range," *Nature Photon.*, vol. 3, pp. 351–356, 2009.
[11] N. Picqué and T. W. Hänsch, "Frequency comb spectroscopy," *Nature Photon.*, vol. 13, pp. 146–157, 2019.
[12] V. Torres-Company et al., "Laser frequency combs for coherent optical communications," *J. Lightw. Technol.*, vol. 37, pp. 1663–1670, Apr. 2019.
[13] International School and Conference on Photonics, Belgrade, Serbia, [Online]. Available: http://www.photonica.ac.rs/index.php
[14] D. Aumiler and T. Ban, "Simultaneous laser cooling of multiple atomic species using an optical frequency comb," *Phys. Rev. A*, vol. 85, 2012, Art. no. 063412.
[15] N. Šantić, D. Buhin, D. Kovačić, I. Krešić, D. Aumiler, and T. Ban, "Cooling of atoms using an optical frequency comb," *Sci. Rep.*, vol. 9, 2019, Art. no. 2510.
[16] D. Buhin et al., "Simultaneous dual-species laser cooling using an optical frequency comb," *Phys. Rev. A*, vol. 102, 2020, Art. no. 021101.
[17] G. Kregar, N. Šantić, D. Aumiler, H. Buljan, and T. Ban, "Frequency-comb-induced radiative force on cold rubidium atoms," *Phys. Rev. A*, vol. 89, 2014, Art. no. 053421.
[18] M. Kruljac, D. Buhin, D. Kovačić, V. Vulić, D. Aumiler, and T. Ban, "Frequency-comb-induced radiation pressure force in dense atomic clouds," *J. Opt. Soc. Amer. B*, vol. 39, pp. 1411–1418, 2022.
[19] Frequency comb cooling of atoms (CoolComb) research project. [Online]. Available: http://cold.ifs.hr/research/frequency-comb-cooling-of-atoms/
[20] C. Weber et al., "Quantum dash frequency comb laser stabilisation by optical self-injection provided by an all-fibre based delay-controlled passive external cavity," *Electron. Lett.*, vol. 55, pp. 1006–1009, 2019.

[21] C. Weber et al., "All-fiber optical-self-injection stabilization of a frequency-comb quantum-dash laser," in *Proc. SPIE*, vol. 11301, 2020, Art. no. 1130120.

[22] A. Delmade, M. Krstić, C. Browning, J. Crnjanski, D. Gvozdić, and L. Barry, "Power efficient optical frequency comb generation using laser gain switching and dual-drive Mach-Zehnder modulator," *Opt. Exp.*, vol. 27, pp. 24135–24146, 2019.

[23] T. Pinto et al., "Optimization of frequency combs spectral-flatness using evolutionary algorithm," *Opt. Exp.*, vol. 29, pp. 23447–23460, 2021.

[24] M. Krstić, J. Crnjanski, M. Banović, I. Vasiljević, and D. Gvozdić, "Generation of a dual optical frequency comb by large signal modulation of a semiconductor laser," *Opt. Lett.*, vol. 46, pp. 4920–4923, 2021.

[25] C. Browning et al., "Gain-switched optical frequency combs for future mobile radio-over-fiber millimeter-wave systems," *J. Lightw. Technol.*, vol. 36, pp. 4602–4610, Oct. 2018.

[26] R. Wu, V. R. Supradeepa, C. M. Long, D. E. Leaird, and A. M. Weiner, "Generation of very flat optical frequency combs from continuous-wave lasers using cascaded intensity and phase modulators driven by tailored radio frequency waveforms," *Opt. Lett.*, vol. 35, pp. 3234–3236, 2010.

[27] Y. Cui, Z. Wang, Y. Xu, Y. Jiang, J. Yu, and Z. Huang, "Generation of flat optical frequency comb using cascaded PMs with combined harmonics," *IEEE Photon. Technol. Lett.*, vol. 34, no. 9, pp. 490–493, May 2022.

[28] T. Ideguchi, A. Poisson, G. Guelachvili, N. Picqué, and T. W. Hänsch, "Adaptive real-time dual-comb spectroscopy," *Nature Commun.*, vol. 5, 2014, Art. no. 3375.

[29] A. M. Zolot et al., "Direct-comb molecular spectroscopy with accurate, resolved comb teeth over 43 THz," *Opt. Lett.*, vol. 37, pp. 638–640, 2012.

[30] T. J. Kippenberg, A. L. Gaeta, M. Lipson, and M. L. Gorodetsky, "Dissipative Kerr solitons in optical microresonators," *Science*, vol. 361, 2018, Art. no. eaan8083.

[31] M. Vainio and L. Hanonen, "Mid-infrared optical parametric oscillators and frequency combs for molecular spectroscopy," *Phys. Chem. Chem. Phys.*, vol. 18, pp. 4266–4294, 2016.

[32] G. Millot et al., "Frequency-agile dual-comb spectroscopy," *Nature Photon.*, vol. 10, pp. 27–30, 2016.

[33] C. Quevedo-Galán, V. Durán, A. Rosado, A. Pérez-Serrano, J. M. G. Tijero, and I. Esquivias, "Gain-switched semiconductor lasers with pulsed excitation and optical injection for dual-comb spectroscopy," *Opt. Exp.*, vol. 28, pp. 33307–33317, 2020.

[34] E. Russell, B. Corbett, and F. C. Garcia Gunning, "Gain-switched dual frequency comb at 2 μm," *Opt. Exp.*, vol. 30, pp. 5213–5221, 2022.

[35] M. Abramowitz and I. A. Stegun, *Handbook of Mathematical Functions With Formulas, Graphs, and Mathematical Tables*, Mineola, New York, USA: Dover Publ. Inc., 1965.